Patterns in the variable Hele-Shaw cell for different viscosity ratios: Similarity to river network geometry

Shashwati Roy and S. Tarafdar
Physics Department, Condensed Matter Physics Research Center, Jadavpur University, Calcutta 700 032, India
(Received 21 February 1996)

This paper reports the generation of interesting viscous fingering patterns in a variable Hele-Shaw cell using a non-Newtonian paint as the displaced fluid. Patterns with infinite and finite ratios of viscosity between the displaced and displacing fluids are produced. We find a qualitative difference between the patterns generated in the two cases. However, displaced fluids of different viscosity generate similar patterns, as long as the viscosity ratio is kept infinite. The infinite ratio of the viscosity of the two fluids produces a paint pattern that exhibits fractal nature. The fractal pattern resembles very much the simulated river basin boundary geometry, which earlier workers have shown to emerge from a minimum energy dissipation principle. [S1063-651X(96)04611-9]

PACS number(s): 47.50.+d, 47.20.−k, 68.10.−m

I. INTRODUCTION

The phenomenon known as viscous fingering (VF), where a fluid of lower viscosity (fluid 2) displaces a fluid of higher viscosity (fluid 1) under pressure, can produce interesting fractal patterns. Fractal growth phenomena and pattern formation appear to be characteristics of many natural processes such as dielectric breakdown, electrochemical deposition, and river network formation [1–3].

A standard apparatus for studying VF is the Hele-Shaw cell. This is an arrangement of two parallel plates separated by a distance of the order of 1 mm, with fluid 1 confined between the plates. Fluid 2 is injected either from one side of a rectangular cell or through a hole at the center of one of the circular plates.

The VF patterns generated in the latter case exhibit radial symmetry. Fractal nature in the patterns is observed in certain length scales, when the two fluids are immiscible [4] or when the fluids are miscible but fluid 1 is non-Newtonian in nature [5].

Another simple method for producing interesting VF patterns is to pull apart two plates with a layer of highly viscous paint sandwiched in between. The surrounding air enters the paint in the form of fingers, producing ultimately a characteristic treelike pattern of paint on both the plates. This is the ''figure ground'' [6] of the complementary VF patterns produced by air. A number of such experiments have already been reported [7–10]. This is referred to as VF in the variable Hele-Shaw cell (VHSC).

The theoretical analysis of structure and stability of a single viscous finger has made steady progress [11,12], but an analysis of the pattern as a whole produced by the competition and interaction of a large number of fingers growing simultaneously is yet to emerge. In this paper we report some works that are expected to be useful for understanding such problems.

To produce a permanent pattern in the VHSC, we use paint as fluid 1. In Sec. II we shall discuss our experimental study, which consists of two parts. In Sec. II A we generate VF patterns, varying the viscosity of the fluid 1 by diluting it with linseed oil in different ratios, fluid 2 being air. In Sec. II B, in a second set of experiments we change the viscosity ratio between fluids 1 and 2 using glycerine as fluid 2. A qualitative explanation for the differences in the patterns is offered in Sec. III. In Sec. IV we discuss the construction of an idealized pattern from the photographs of the real VF patterns and show that it is remarkably similar to simulated river networks [13] that are based on a minimum energy dissipation principle. We summarize in Sec. V.

II. EXPERIMENTAL STUDY OF THE PATTERNS

A. Set 1

We press two glass slides together with a drop of paint in between. The paint spreads out to form a thin layer having an almost circular boundary. The slides are now separated manually keeping them parallel as far as possible. The undiluted paint is a highly viscous non-Newtonian fluid (Camlin Students oil paint, cadmium yellow) as reported earlier [10]. We now repeat the experiment diluting the paint with linseed oil in different ratios. Figure 1 shows patterns for paint-to-oil ratios 1:0.0 and 1:1.8. The viscosity η of the paint-oil mixture vs the velocity gradient D is shown for different dilutions in Fig. 2.

As dilution increases the tree patterns formed by the oil-paint mixtures become broader compared to the undiluted paint pattern. The relative area occupied by the paint increases with dilution. However, the overall appearance remains the same, branching angles and the average number of fingers meeting at the center remaining more or less unaffected.

The characteristic features of VF patterns depend more on the viscosity ratio between fluid 1 and fluid 2 than the absolute coefficient of viscosity of one component [14]. So the overall similarity in set-1 patterns is quite expected. The paint is diluted with linseed oil of viscosity $\eta = 33.1$ cp at 30 °C, so the effective viscosity is still very large compared to air ($\eta \sim 0$).

B. Set 2

To observe the effect of a finite viscosity ratio, we undertake a second set of experiments where fluid 2 is glycerine,

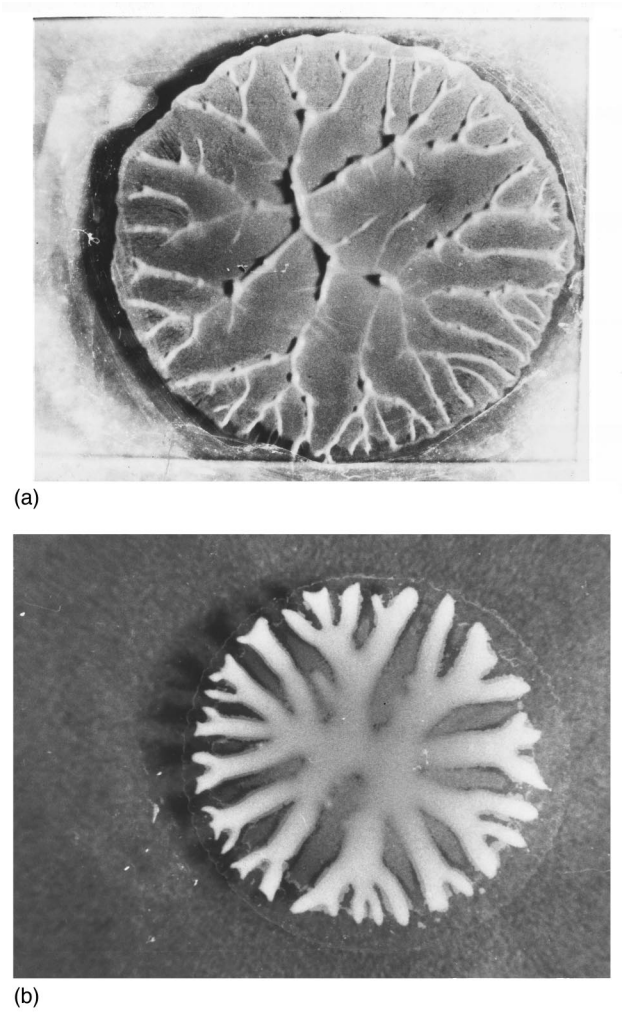

FIG. 1. Two patterns generated in set-1 experiments (a) with undiluted paint and (b) with a paint-to-oil ratio 1:1.8. The branches of the tree pattern of paint in (a) are elevated as they reach the center, which is evident from the shadow, while the branches in (b) widen.

$\eta = 629$ cp at 30 °C, and fluid 1 is undiluted paint. The procedure now is simply to separate the glass slides submerged in a trough filled with glycerine.

We find that under glycerine, the glass slides cannot be separated manually while keeping them parallel, the force required being very large. So a slightly different procedure is adopted. The upper slide is replaced by a circular cover slip and the lifting is done by inserting a pin at the edge of the cover slip as in our previous report [10]. The patterns are shown in Fig. 3, which include, for comparison, the undiluted paint–air pattern generated by an exactly similar lifting process.

In the case of a finite viscosity ratio the patterns are qualitatively different. The glycerine fingers grow almost parallel and there is very little branching in the tree pattern, unlike the paint-air situation.

III. QUALITATIVE EXPLANATION OF THE DIFFERENT VF PATTERNS

The schematic diagrams of the initial random fluctuations and the three types of patterns obtained for pure paint and air, diluted paint and air, and pure paint and glycerine are shown in Figs. 4(a)–4(d). We suggest a qualitative explanation for the differences observed. A linear geometry is shown, valid at the periphery of any of our patterns. An initial random fluctuation is shown in Fig. 4(a). This may be due to unevenness of the surface or thermal fluctuation.

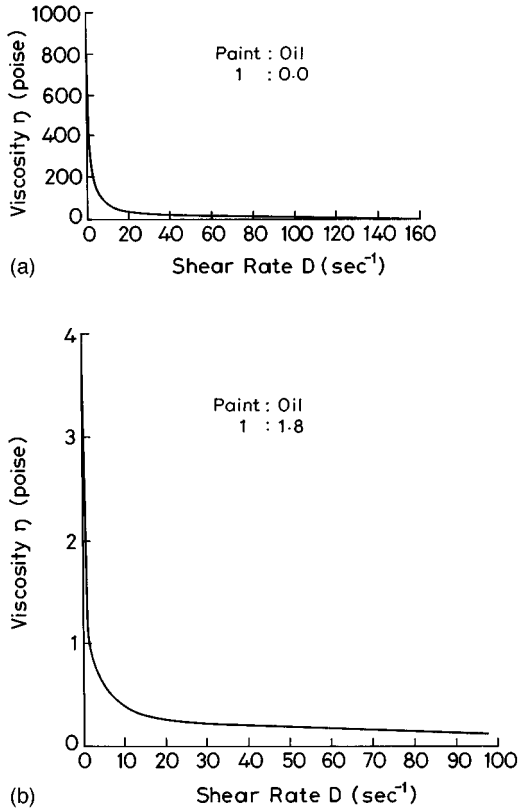

FIG. 2. Plot of viscosity of the paint-oil mixture, η vs shear rate D for a paint-to-oil ratio (a) 1:0 by volume and (b) 1:1.8 by volume.

When air enters at a constant pressure P_o at the periphery we assume a constant lower pressure P, well within the paint [Fig. 4(b)]. Now the pressure gradient at the tip of a longer air finger is larger than that at the tip of a shorter finger [2]. According to Darcy's law, the velocity is proportional to the pressure gradient, so a longer finger moves more rapidly than a shorter finger. The air spreads out forward as well as laterally since fluid 1 is of much higher viscosity and so pressure cannot transmit fast through it and the lateral growth of a longer finger continues until pressure in the adjacent longer finger balances, as shown in Fig. 4(b).

In Fig. 4(c) fluid 1 is diluted paint and the situation is similar to the previous one. The only difference is that fluid 1 is less viscous than in the previous case, pressure is transmitted through it faster, and the lateral pressure in the adjacent longer finger balances it faster than in the earlier situation, resulting in a thicker wall of paint between two air fingers.

In Fig. 4(d) the fluid 2 is also of finite viscosity and hence pressure inside the glycerine finger is not constant at P_o but decreases with distance l from the periphery. We assume a linear fall in pressure, i.e., P (at l) $= P_o - l\overline{\nabla P}$, where $\overline{\nabla P} = (P_o - P)/L$. Then the pressure gradient at point A, the

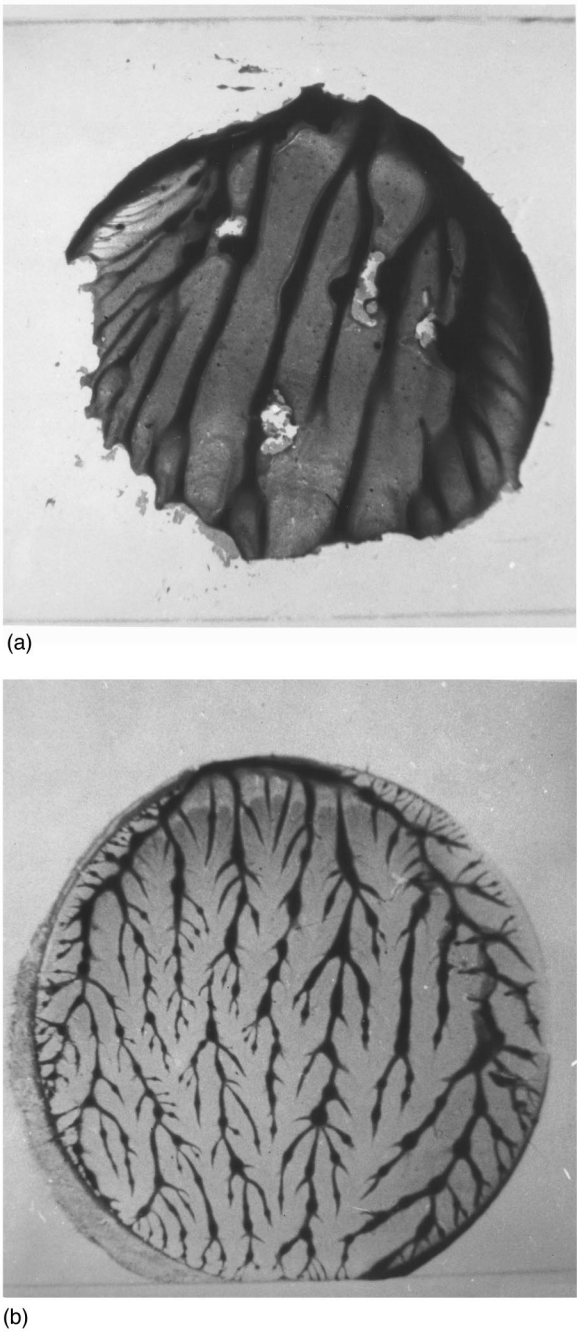

(a)

(b)

FIG. 3. Two patterns generated in set-2 experiments. Displacing fluids are (a) glycerine and (b) air, respectively. Displaced fluid is undiluted paint in both cases.

tip of a longer finger, and that at B, the tip of a shorter finger, will be equal since

$$\nabla P_A=[P_o-(L-x_1)\overline{\nabla P}-P]/x_1 = \nabla P_B=[P_o-(L-x_2)\overline{\nabla P}-P]/x_2 . \quad (1)$$

This indicates that in spite of differences in the length of glycerine fingers at the initial stage, all of them proceed with the same velocity, remaining almost parallel to each other.

IV. SIMILARITY TO SIMULATED RIVER PATTERNS

Sun, Meakin, and Jossang simulate a river network [13] on a rectangular island surrounded by the sea, using the minimum energy dissipation principle. A triangular lattice is superposed on the island and a unit precipitation on each lattice site is assumed with the condition that the river network transports the total precipitation from the island to the sea. Each site on the boundary of the lattice has a possibility of being a channel network outlet. The entire area from which water drains out through a single site on the boundary constitutes a basin. So each basin contains a single river with tributaries.

In our set-1 experiments air enters through the boundary of a circular area displacing a uniform distribution of paint over the area. Ultimately, when the slides are separated air is distributed uniformly over the entire area with a tree pattern of paint, which separates different air fingers. So the process is just the reverse of the river network formation. A single air finger corresponds to a single river network and the paint pattern corresponds to the basin boundary pattern. Experimentally obtained tree patterns show a striking similarity to the basin boundary geometry [Fig. 4(d) in [13]]. To see the resemblance, the branches formed inside the tree pattern that do not reach the boundary must be excluded. Both exhibit a loopless fractal nature on certain length scales [13,10]. The average number of air fingers meeting at the center of the VF pattern is more or less the same as the number of large basins joined together at the center of the island.

To bring out the similarity and analyze the VF patterns in detail we construct an idealized hexagonal model of the tree pattern on a triangular lattice, as shown in Fig. 5. The model is based on some statistical data of the real VF patterns, namely, the average number of air fingers ultimately reaching the center, the hierarchical structure of air fingers, and the equal width of air fingers at the boundary and equal branching angles. Only the side branching and tip splitting of the air fingers are ignored.

The cumulative distribution of air finger area, as in Fig. 5, follows a power law

$$N(A>A^*)\propto A^{-\beta}, \quad (2)$$

with $\beta=\frac{1}{2}$. $N(A>A^*)$ is the number of air fingers of area greater than A^*. The value of the exponent β is the same as the exponent $(\tau-1)$ given in Ref. [13]. This is also expected from the simple scaling argument [13] as the air fingers in VF patterns are compact in nature.

According to Sun, Meakin, and Jossang, energy dissipation at ith link,

$$P_i\propto L_i Q_i^{\alpha}, \quad (3)$$

where L_i is the length of the ith link and Q_i is the amount of water flow at the ith link and $\alpha=\frac{1}{2}$. We assume that the same relationship holds for the reverse case, i.e., energy dissipation for drawing air inside is also proportional to $Q_i^{1/2}$, Q_i representing the amount of air drawn inside, and hence the model pattern can also be obtained using the relation (3) and minimizing $P=\Sigma P_i$, the total energy dissipation.

The study of the branching structure of a single tree reveals that sidebranching is preferred to tip splitting for air

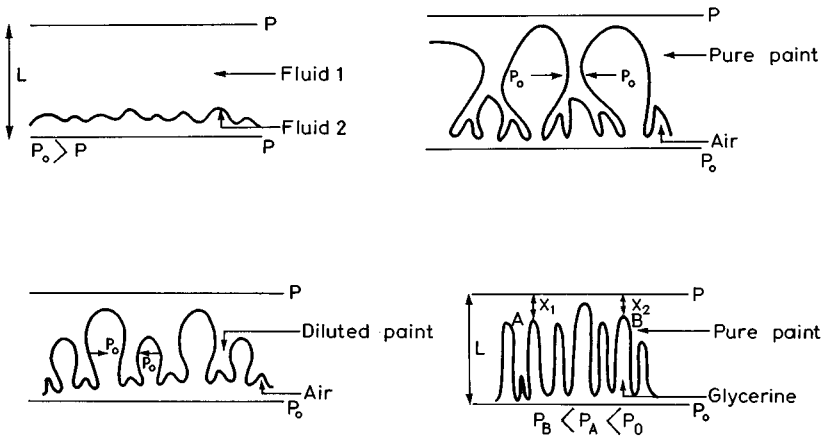

FIG. 4. Schematic diagram of (a) an initial random fluctuation at the two-fluid interface in a linear Hele-Shaw cell of length L, (b) growth of large air fingers suppressing some other fingers in the forward and lateral directions through undiluted paint, (c) growth of almost all air fingers through diluted paint, and (d) growth of parallel glycerine fingers in the forward direction through undiluted paint.

fingers (the typical nature of tributaries of a single river network is similar). To reveal the significance of the exponent α and relate it to the branching structure of each tree, we show explicitly how relation (3) works in a small air ''basin'' of the model tree pattern. The air enters through any one of the two lattice sites, at which the basin opens at the boundary, and the amount of air is measured by the number of lattice sites within the small basin selected. We impose the condition that the final distribution of air will be such that at each lattice site there will be one ''unit'' of air. No backward movement of air is allowed. Using these conditions, all possible air flow paths within the basin and the corresponding energy dissipation are calculated.

The minimum energy dissipation corresponds to the path shown in Fig. 6(a). Figure 6(b) shows another path with higher dissipation energy. These two air flow paths indicate that the tree pattern that obeys minimum-energy dissipation principle is really generated by sidebranching rather than tip splitting of air finger, as also observed in the real VF patterns. Fractional values of $\alpha<1$ signify that air prefers to flow together as far as possible. It is to be noted that the paths in Figs. 6(a) and 6(b) give the same P for $\alpha=1$. In this case it is immaterial whether or not the fluid units flow together. Each unit tries to minimize its path independently. On the other hand, $\alpha=0$ implies that the total length of the pattern should be minimized. We propose that, in our problem, the viscosity ratio and the interfacial tension between fluids 1 and 2 determine α. The two extreme limits $\alpha=0$ and 1, correspond, respectively, to the cases where only interfacial tension controls the flow of air and the situation when viscous force plays the dominating role. The actual pattern arises from the interplay of these two competing forces, giving an intermediate fractional value of α.

V. CONCLUSION

To summarize, we have seen the effect of varying the viscosity of fluid 1 and the viscosity ratio between fluids 1 and 2, on the VF patterns in a VHSC. We have also observed the similarity in patterns generated in our set-1 experiments with another natural process: river network formation. The last part leads to the question whether natural processes exhibit self-organization according to some global energy-minimization principle [15]. The VHSC would be a convenient model for probing this question further.

Another theoretical work, by Sarkar [16], suggests an idealized radial VF pattern in conventional Hele-Shaw cells for immiscible fluids. The suggested pattern is complementary

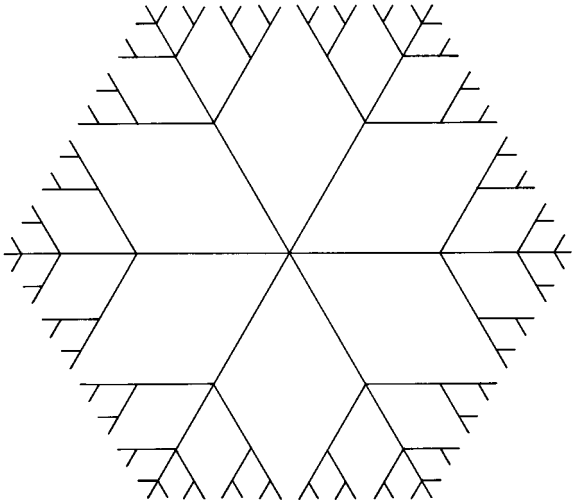

FIG. 5. Idealized hexagonal model of the tree pattern obtained in set-1 experiments with undiluted paint.

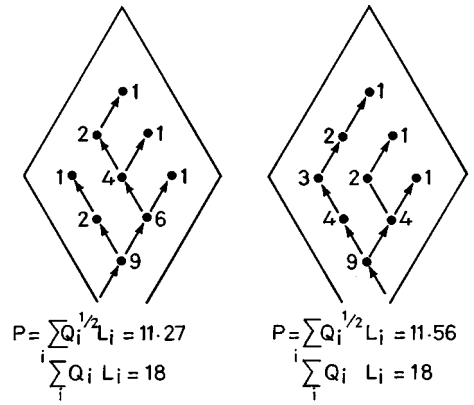

FIG. 6. Air flow path within a small air ''basin'' of the model tree pattern. Path (a) corresponds to the minimum value of P and path (b) gives the same $\Sigma L_i Q_i$ as (a), but P is higher than in (a).

to ours. He used an effective-medium approximation to explain the scaling behavior in the patterns.

We plan to generate the whole tree pattern through computer simulation and investigate thoroughly the dependence of α on the surface tension and viscosity through experiments and theory. Another aspect of our experiment that requires analysis is the effect of the non-Newtonian nature of fluid 1 on the VF patterns; we plan to study this in detail.

ACKNOWLEDGMENTS

The authors wish to thank J. Roy for photographing the patterns; Professor S. Sengupta, Professor A. N. Basu, and Dr. T. R. Middya for encouraging discussions; and the Polymer Science Unit, led by Professor B. Mondol, IACS, Calcutta-32, for help in the viscosity measurement. S. R. thanks the State Government of West Bengal for financial support.

[1] B. B. Mandelbrot, *The Fractal Geometry of Nature* (Freeman, New York, 1983).
[2] J. Feder, *Fractals* (Plenum, New York, 1988).
[3] P. Meakin, Rev. Geophys. **29**, 335 (1991).
[4] S. N. Rauseo, P. D. Barnes, Jr., and J. V. Maher, Phys. Rev. A **35**, 1245 (1987).
[5] G. Daccord, J. Nittman, and H. E. Stanley, Phys. Rev. Lett. **56**, 336 (1986).
[6] D. R. Hofstadter, *Gödel, Escher and Bach: An Eternal Golden Braid* (Vintage, New York, 1979).
[7] E. Ben-Jacob, R. Godbey, N. D. Goldenfeld, J. Koplik, H. Levine, T. Muller, and L. M. Sander, Phys. Rev. Lett. **55**, 1315 (1985).
[8] H. La Roche, J. F. Fernandez, M. Octavio, A. G. Loeser, and C. J. Lobb, Phys. Rev. A **44**, R6185 (1991).
[9] J. Bohr, S. Brunak, and T. Norretranders, Europhys. Lett. **25**, 245 (1994).
[10] S. Tarafdar and S. Roy, Fractals **3**, 99 (1995).
[11] D. Bensimon, L. P. Kadanoff, S. Liang, B. I. Shraiman, and C. Tang, Rev. Mod. Phys. **58**, 977 (1986).
[12] D. C. Hong and J. S. Langer, Phys. Rev. Lett. **56**, 2032 (1986); R. Combescot, T. Dombre, V. Hakim, Y. Pomeau, and A. Pumir, *ibid.* **56**, 2036 (1986).
[13] T. Sun, P. Meakin, and T. Jossang, Phys. Rev. E **49**, 4865 (1994).
[14] J. V. Maher, Phys. Rev. Lett. **54**, 1498 (1985).
[15] A. Rinaldo, I. Rodriguez-Iturbe, R. Rigon, E. Ijjasz-Vasquez, and R. L. Bras, Phys. Rev. Lett. **70**, 822 (1993).
[16] S. K. Sarkar, Phys. Rev. Lett. **65** 2680 (1990).